Article

Stratigraphic Constraints on Sandy Conglomerates in Huanghekou Sag, Bohai Bay Basin, via In Situ U-Pb Dating of Vein Calcite and Detrital Zircons, and XRD Analysis

Wei Wang [1,2,*] **, Xianghua Yang** [1,2,*] **, Hongtao Zhu** [1,2] **and Li Huang** [1,2]

1   School of Earth Resources, China University of Geosciences, Wuhan 430074, China; htzhu@cug.edu.cn (H.Z.); 1202020021@cug.edu.cn (L.H.)
2   Key Laboratory of Tectonics and Petroleum Resources, Ministry of Education, China University of Geosciences, Wuhan 430074, China
*   Correspondence: wang.wei@cug.edu.cn (W.W.); xhyang@cug.edu.cn (X.Y.)

Abstract: The discovery of the BZ19-6 large-scale condensate gas field illustrates the great potential of the sandy conglomerate reservoirs in the Bohai Bay Basin. However, the stratigraphic correlation of the sandy conglomerate sequence in northern Huanghekou Sag remains a challenge due to the lack of syn-depositional volcanic layers and biostratigraphic constraints. The challenge limits understanding the regional strata distribution and further exploration deployment. In this study, we conducted in situ U-Pb dating of vein calcite and detrital zircons of the sandy conglomerate samples from borehole BZ26-A. The vein calcite age and the youngest age of detrital zircons provide the upper and lower bounds of the depositional age, respectively. We also correlated the samples with those from well-understood strata through a comparison of XRD mineral components. The absolute age of 47.0 Ma of the vein calcite and the youngest detrital zircon age of 103.5 Ma suggest the sedimentary sequence is supposed to be referred to as the Kongdian Formation (65–50.5 Ma). The XRD data and petrological analysis suggest that the lithostratigraphy of the Kongdian Formation in Huanghekou Sag could be divided into at least three members, with Member 3 consisting of red sediment deposited in a hot and dry climate; Member 2 and Member 1 deposited as fan delta with major parent rock of Mesozoic volcanic rocks and Precambrian meta-granitoid, respectively. Member 1 shows significant potential for energy exploration due to high brittle mineral components and fracture development.

Keywords: sandy conglomerate; Huanghekou Sag; stratigraphic correlation; calcite U-Pb dating; detrital zircon

1. Introduction

The potential of the sandy conglomerate sequence as reservoirs has been proved by the discovery of the BZ19-6 large-scale condensate gas field in Bozhong Sag, Bohai Bay Basin, China, with reserves exceeding 100 billion cubic meters. The success lights the progress in studies of the sandy conglomerate in the Paleocene Kongdian Formation [1,2]. This is the first time large-scale thick fractured-porous sandy conglomerate reservoirs in the Kongdian Formation in Bohai Bay Basin have been discovered, which breaks through the previous forbidden area of deep-buried sandy conglomerates and greatly expands the exploration field of Paleogene oil and gas [1]. However, understanding the stratigraphic distribution of the sandy conglomerate sequence remains a challenge due to the interpretation ambiguity of deep seismic data (>3500 m), paucity of biostratigraphic information, and lack of reference laminae, such as mudstone or volcanic layers [3,4]. These characteristics limit the exploration process, especially in expanding the area from Bozhong Sag to the Huanghekou Sag in the south (Figure 1). Thus, new methods of stratigraphic correlation and further understanding of the Kongdian Formation are needed for future exploration.
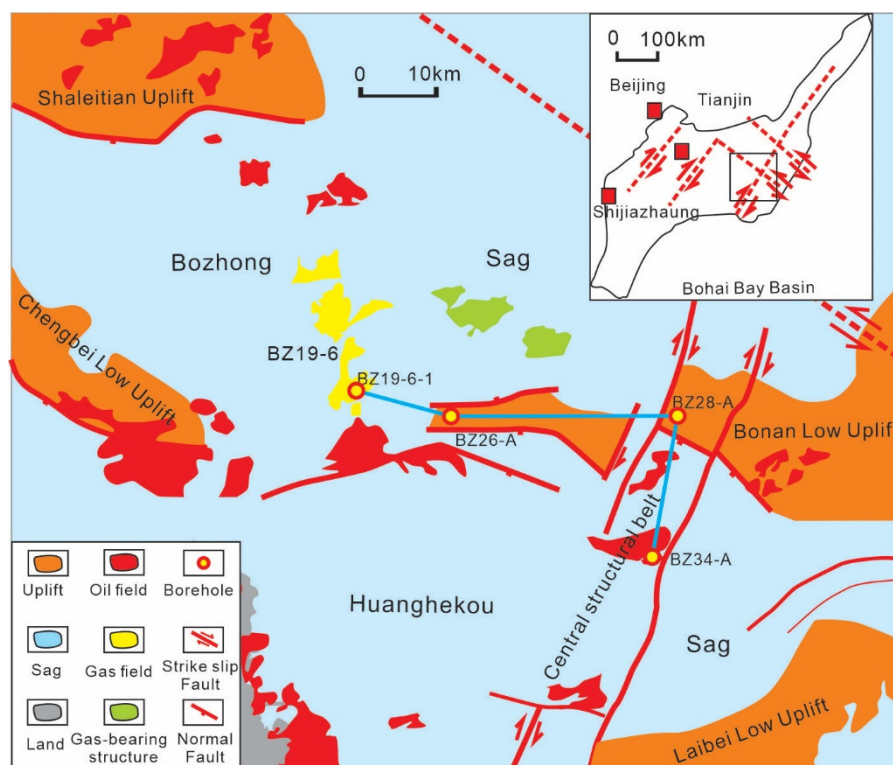
Figure 1. Geological map of the study area showing major tectonic elements, oil-gas bearing structures, and boreholes.

Although U-Pb dating of carbonate minerals, such as calcite and dolomite, is technically challenging due to low U concentrations (<10 ppm), the technique has been developing fast and is widely used in studies on carbonate diagenesis and brittle faulting in recent years [5–7]. However, the powerful method, which could provide the absolute time of precipitation of carbonate minerals, is seldom used in studies on clastic rocks. On the contrary, detrital zircon geochronology is widely used to constrain the maximum depositional age of a clastic unit, where the youngest age component provides the earliest possible age of deposition [8–10]. Since carbonate, especially calcite veins and detrital zircons, are widespread in sedimentary rocks, in this study, we try to conduct stratigraphic correlation through the in situ U-Pb dating of both vein calcite and detrital zircons, which provide the upper and lower bounds of the depositional age of the host rock, respectively. In addition, we also conducted XRD major and clay mineral analysis on the inter-gravel matrix of the sandy conglomerate samples. The mineral components containing information on parent rocks, diagenetic process, and paleoclimate were used for further correlation. The results could strengthen the understanding of the Kongdian Formation in the Bohai Bay Basin and shed light on similar correlating work in other areas.

2. Geological Setting

The Bohai Bay Basin is a significant hydrocarbon-bearing offshore basin located in Eastern China, which developed on the North China Block under the control of both Cenozoic rifting and strike-slip tectonics, along the Tan-Lu Fault Zone (Figure 1) [11,12]. The Paleocene of the basin can be divided into Kongdian, Shahejie and Dongying Formations (Figure 2), with stratigraphic data from the drilled values and bottom ages from the Editorial Committee of Petroleum Geology of China (1987) [13]. The Kongdian Formation ($E_{1-2}k$, bottom age of 65 Ma) and the fourth member of the Shahejie Formation (E_2s_4, bottom age of 50.5 Ma) were deposited in the initial extensional stage from the Paleocene to early Eocene. The deposition is characterized by fan delta sandy conglomerates and shallow lacustrine gray mudstones, accompanied by alluvial fan and lacustrine red conglomerates

and mudstones [2,14]. The third member of the Shahejie Formation (E_2s_3), with a bottom age of 42 Ma, deposited during the early Eocene, is characterized by middle to deep lacustrine facies, with local fan delta deposits [13,15] Member two (bottom age of 38 Ma) to member one (bottom age of 36 Ma) of the Shahejie Formation ($E_2s_2 \sim E_2s_1$) are deposited under a relatively stable tectonic setting with deposition of lacustrine mudstones and fan delta pebbly sandstones. The Dongying Formation (E_3d), deposited during the Oligocene, was characterized by shallow lacustrine fine sandstones, interbedded with gray mudstones and delta plain pebbly sandstones interbedded with mudstone [13,15].
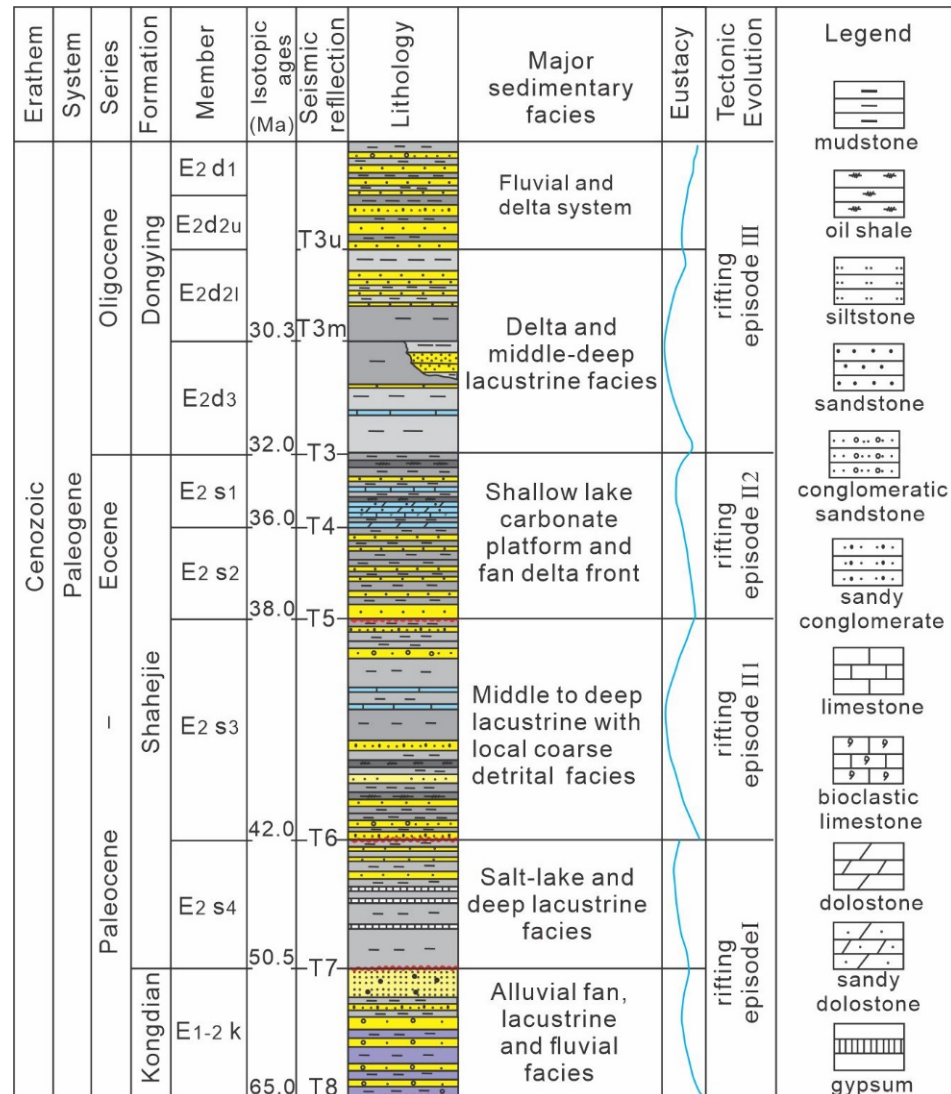
Figure 2. Generalized Cenozoic stratigraphy, facies, and tectonic events and stages of the Bohai Bay Basin.

The BZ19-6 Structure of Bozhong Sag, located between the Chengbei Low Uplift and the Bonan Low Uplift in the southwestern Bohai Sea (Figure 1), is an anticline where the Kongdian Formation is widely distributed. The major reservoirs of the Kongdian Formation are sandy conglomerates deposited in fan delta facies [1], accounting for an important part of the super-huge condensate oil field, with reserves of over 100 billion m^3 [1,2]. To the south of the BZ19-6 structure, the southern steep slope zone of the Bonan Low Uplift is a successive area for the exploration of deep-buried strata from Bozhong Sag to Huanghekou Sag, but with an ambiguous understanding of the stratigraphic distribution. BZ26-A is the only structure with boreholes and cores in this area (Figure 1), which uncovers a thick

sandy conglomerate sequence with uncertain depositional ages due to a lack of biostratigraphic data and syn-depositional volcanic layers [16]. The absence of distinguishable sporopollen and reference lamina limits the understanding of the borehole and further strata distribution.

Fortunately, three intervals in the sandy conglomerates were cored from the borehole BZ26-A (Figure 3). The sedimentary and petrologic analysis suggests the sediment was deposited as a fan delta facies. In these intervals, abundant tectonic fissures developed and were partly filled with secondary minerals [16]. The C2 core interval shows the development of calcite veins filling parts of the tectonic fissures (Figure 4A). In the east, boreholes BZ28-A and BZ34-A were drilled into the Kongdian Formation on the Bonan Low Uplift and Central Structural Belt [14,15], respectively, due to relatively shallow buried depths on structural highs (Figures 1 and 3). Two intervals were cored from the conglomerate interval (~400 m in thickness) of BZ28-A. The core D1 consists of yellow-grey sandy conglomerates, while D2 shows a red to brown color (Figure 3). One interval was cored from borehole BZ34-A, which shows red to brown mixed mud and gravels (Figure 3). Both the boreholes revealed red to brown sediments (D2 and E1), which are considered reference lamina of the Kongdian Formation in the Bohai Bay Basin [14,17].
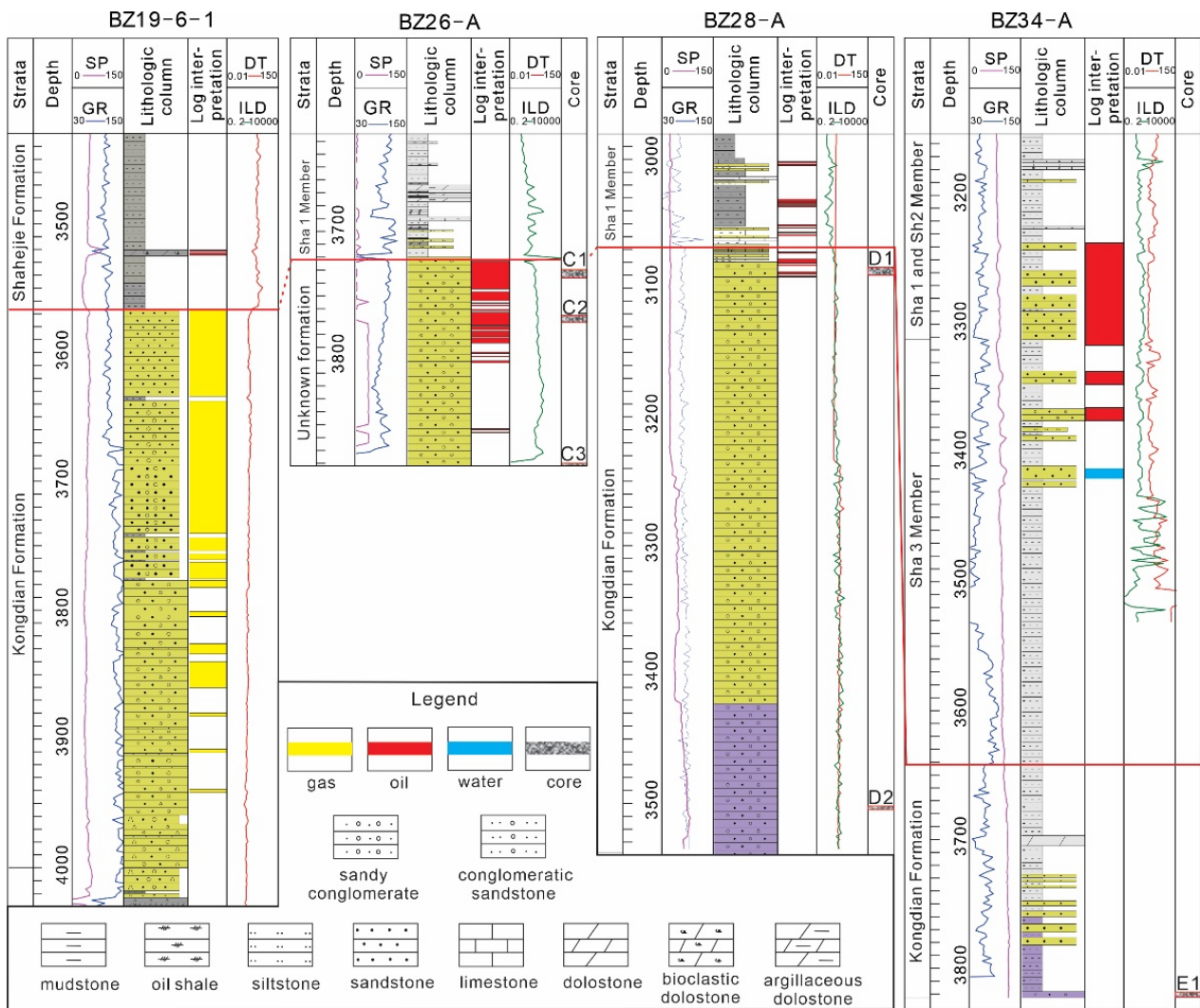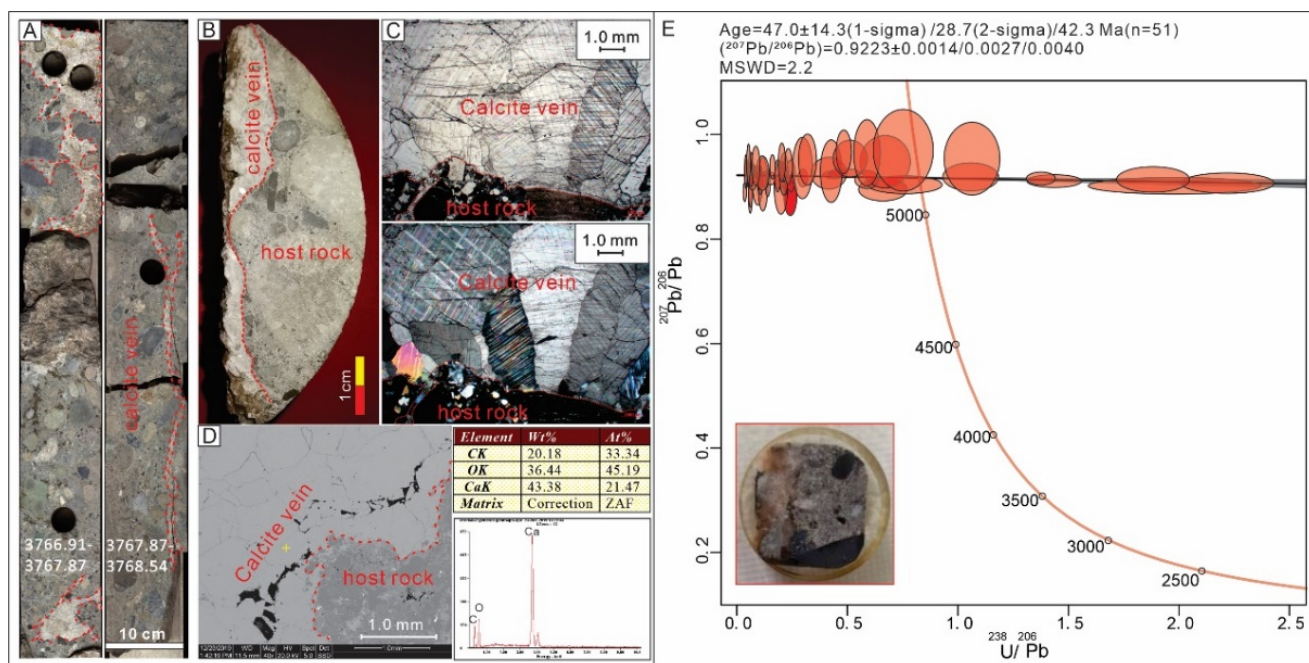

Figure 3. Stratigraphic section showing the borehole lithologies and the positions of sequence boundaries and core intervals.

Figure 4. (**A**) Photos of part of the C2 core, BZ26-A with vein calcite marked; (**B**) photo of core showing contact relation of calcite vein and wall rock; (**C**) calcite vein micrographs under polarized (upper) and orthogonal light(lower); (**D**) back-scattering image of calcite vein and wall rock with residual pore and energy spectrum (EDS); (**E**) the chosen 2.5 cm-diameter mount of calcite vein and Tera-Wasseerburg $^{238}U/^{206}Pb$-$^{207}Pb/^{206}Pb$ Concordia plot for the vein calcite sample.

3. Sample and Method

3.1. In Situ U-Pb Dating of Vein Calcite

We collected four samples of calcite veins developed in the host rock of the sandy conglomerate sequence from the core C2 of borehole BZ26-A (Figure 3). Observation of cores, thin section analysis, and backscattered electron images with EDS show relatively homogeneous calcite filling the tectonic fissures of the host rock (Figure 4A–D).

LA-ICP-MS elemental pre-screening and in-situ U-Pb dating were conducted at the Radiogenic Isotope Facility, the University of Queensland, Australia. The four samples went through a lapidary process and were made into 2.5 cm diameter mounts (Figure 4E) and then assembled into a Laurin Technic sample holder for pre-screening for ^{238}U, ^{232}Th, ^{208}Pb, ^{207}Pb, ^{206}Pb ion beams and other key major and trace elements. In-situ element analysis was conducted using an ASI RESOlution SE 193 nm ultraviolet (UV) ArF-Excimer laser ablation system coupled with a Thermo I Cap-RQ quadrupole ICPMS. Laser repetition rate and energy levels were set to 15 Hz and 3 J/cm^2, respectively. The diameter of the laser spot was 100 μm. NIST-612 glass standard was employed for normalization and ^{43}Ca was used as an internal standard. The data were processed via Iolite software [18]. Areas with a range of $^{238}U/^{206}Pb$ correlated with $^{207}Pb/^{206}Pb$, possibly defining a reference lower-intercept age on the Tera-Wassenburg Concordia diagram, were chosen as suitable for following U-Pb dating. Areas with low U/Pb ratios or extremely low U were excluded.

Further, 200 μm diameter spots were selected around the locations where high U/Pb ratios had been detected for the subsequent U/Pb dating. NIST-614 glass standard was used to correct for $^{207}Pb/^{206}Pb$ fractionation and instrument drift in the $^{238}U/^{206}Pb$ ratio. Typical sensitivity achieved was ~180,000 cps/ppm ^{238}U.

A matrix-matched calcite standard, AHX-1D (238.2 ± 1.5 Ma U-Pb age), was used to correct for matrix-related bias in $^{238}U/^{206}Pb$ ratios (unpublished). Another calcite standard of PDTK-2 (153.7 ± 1.7 Ma by isotope dilution, unpublished) was used as secondary reference material to ensure accuracy. Raw data were processed to obtain a range of

^{238}U/^{206}Pb and ^{207}Pb/^{206}Pb ratios, which may define a lower-intercept age on the Tera-Wassenburg Concordia diagram using the online version of IsoplotR of Vermeesch [19]. Uncertainties of calculated ages were reported at the 2σ level. During the period when our samples were measured, AHX-1D and PTKD-2 standards gave lower-intercept ages of 255.5 ± 2.2 Ma and 158.0 ± 2.1 Ma, respectively.

3.2. U-Pb Dating of Detrital Zircon

We collected one sample from the C2 core interval (3770.36–3770.56 m) of borehole BZ26-A and separated it using standard mechanical, heavy liquids, and electromagnetic mineral separation techniques. Zircon grains were picked under a binocular microscope, mounted in epoxy, and polished for U-Pb spot analyses. Cathodoluminescence (CL) images were used to evaluate the internal structure of grains, so that grains with inclusions and/or fractures were excluded from our analysis. U-Pb dating of zircons was conducted by LA-ICP-MS at the Micro-Macro Geochemistry Technology (Langfang) Co., Ltd., Langfang, China. Laser sampling was performed using a NewWave UP-213 Nd: YAG solid-state laser. An Agilent 7900 ICP-MS instrument was used to acquire ion-signal intensities.

During the test, helium is used as carrier gas and argon as compensation gas to adjust the sensitivity. They are mixed and connected to ICP-MS through a T-connector. The spot size of the laser was set to 30 μm. The energy density and frequency were set to 10 J/cm^2 and 10 Hz. NIST SRM610 was used to yield the highest sensitivity, lowest oxidation, background, and stable signal to achieve optimal condition. Standard zircon 91,500 was used as the external standard for isotope ratio correction [20], and standard zircon Plesovice (337 Ma) was used as the monitoring blind sample [21]. We Use GLITTER 4.0 software to calculate isotope ratio and element content.

3.3. X-Raydiffraction (XRD) Analysis of Bulk Rocks and Clay Minerals

Nine samples from C1, C2, and C3 intervals of BZ26-A were collected for XRD major mineral analysis with six of them for further clay mineral analysis. Five samples from the D1 and D2 core intervals of BZ28-A, and two samples from the E1 core interval of BZ34-A, were collected for XRD major and clay mineral analysis for comparison. The details of sampling sites and depths are available in Table S3 in the Supplementary Materials.

Samples were crushed into pieces and gravels were artificially excluded. Rock pieces were ground with an agate mortar until the total particle size was less than 300 mesh (48 microns). The mineralogy of the bulk rock and the clay minerals prepared by the side-loading method was carried out by X-ray diffraction (XRD) using an X-ray diffractometer (SmartLab SE). The mineral compositions and their relative proportions of the bulk rocks and clay minerals in the purified clay samples were obtained using the Clayquan (2018 version) program. The XRD analysis covers minerals of quartz, K-feldspar, plagioclase, calcite, dolomite, siderite, pyrite, hematite, laumontite, anhydrite augite, ankerite, and total clay minerals. The clay minerals were further analyzed for division of illite, kaolinite, chlorite, illite/smectite mixed layer, and chlorite/smectite mixed layer.

4. Results

4.1. InSitu U-Pb Dating of Vein Calcite

In-situ element analysis of 165 spots with a diameter of 100 μm was conducted for pre-screening. The results show a ubiquitously low concentration of ^{238}U, less than 0.01 ppm. Four spots from sample 1 with relatively higher ^{238}U of 0.02–0.27 ppm were chosen for further in situ dating. The result of 51 valid 66 U-Pb dating spots shows a narrow range of ^{238}U/^{206}Pb that is correlated with ^{207}Pb/^{206}Pb, defining a reference lower-intercept age on the Tera-Wassenburg Concordia diagram of 47 ± 14.3 Ma (1 sigma), with relatively large uncertainty (Figure 4E). The complete dataset is available in Table S1 in the Supplementary Materials.

4.2. U-Pb Dating of Detrital Zircon

Of the 240 detrital zircon grains analyzed from the core sample, a total of 235 grains yielded U-Pb ages within the concordant criteria (>80%). In general, the sample contains major groups of Late Archean to Early Proterozoic (~2500 Ma), Late Early Proterozoic (~1900–1800 Ma), and Late Mesozoic (150–100 Ma) and a minor group of Late Paleozoic to Early Mesozoic (~200–350 Ma). The youngest zircon with an age of 103.5 ± 2.5 Ma shows typical oscillatory zoning (Figure 5). The complete dataset is available in Table S2 in the Supplementary Materials.
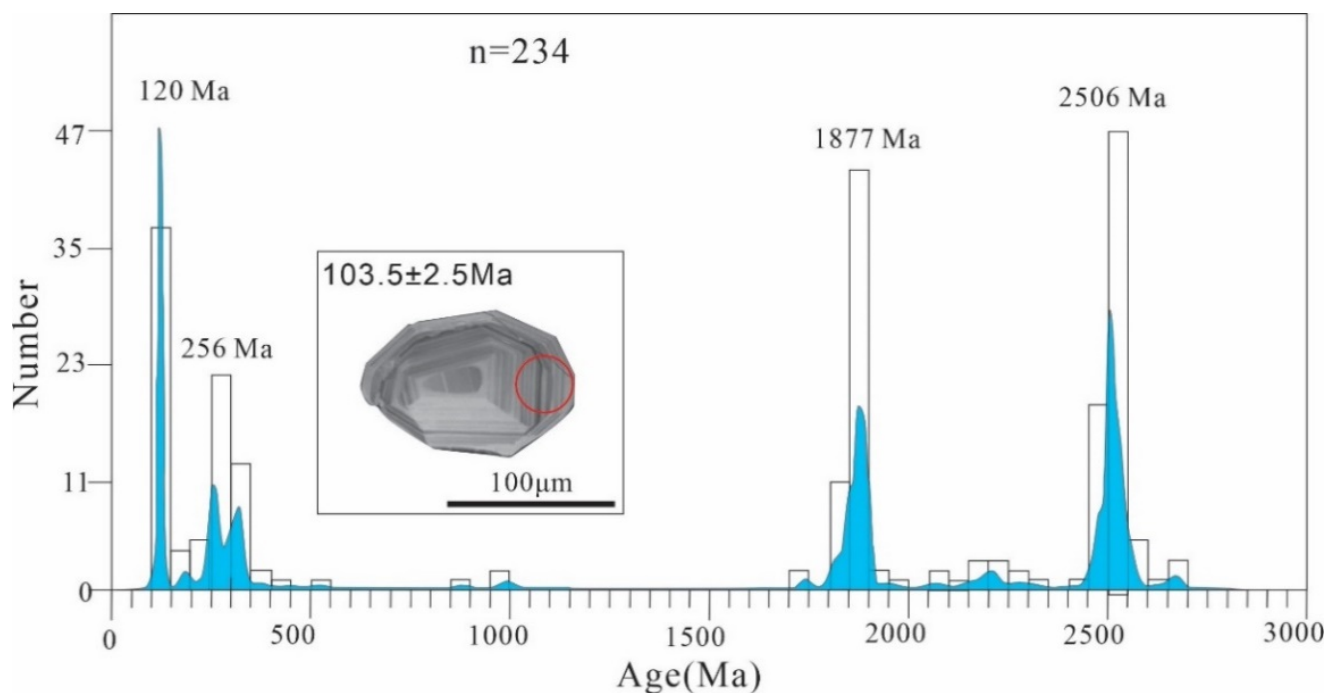

Figure 5. Kernel density estimation plot [22] of detrital zircon U-Pb ages of the sample from C2 core of borehole BZ26-A and CL image of the youngest zircon grain where the red circle marks the site of LA-ICPMS analysis. Data are discretized at a fixed interval (50 Ma).

4.3. XRD Analysis

The inter-gravel matrix of the sandy conglomerate is mainly composed of quartz, K-feldspar, plagioclase, augite, hematite, and clay minerals, which were converted into 100% and plotted (Figure 6). Six samples from cores C1 and C2 show similar components with dominant quartz (>60%), almost absent plagioclase, and approximately similar amounts of K-feldspar, augite, and clay minerals (less than 10%), respectively. Mineralogy of C3 and D1 is characterized by the occurrence of plagioclase, accounting for over ~20% and samples from red to brown cores of D2 and E1 show 4–6% hematite. The complete dataset is available in Table S3 in the Supplementary Materials.

The clay minerals are composed mainly of I/S (illite/smectite mixed layer), illite, kaolinite, and chlorite. Clay minerals of samples from cores C1 and C2 are mainly composed of I/S and illite. Samples from C3, D1, and D2 cores show high amounts of chlorite and kaolinite, while E1 is characterized by dominant I/S and illite (Figure 6).
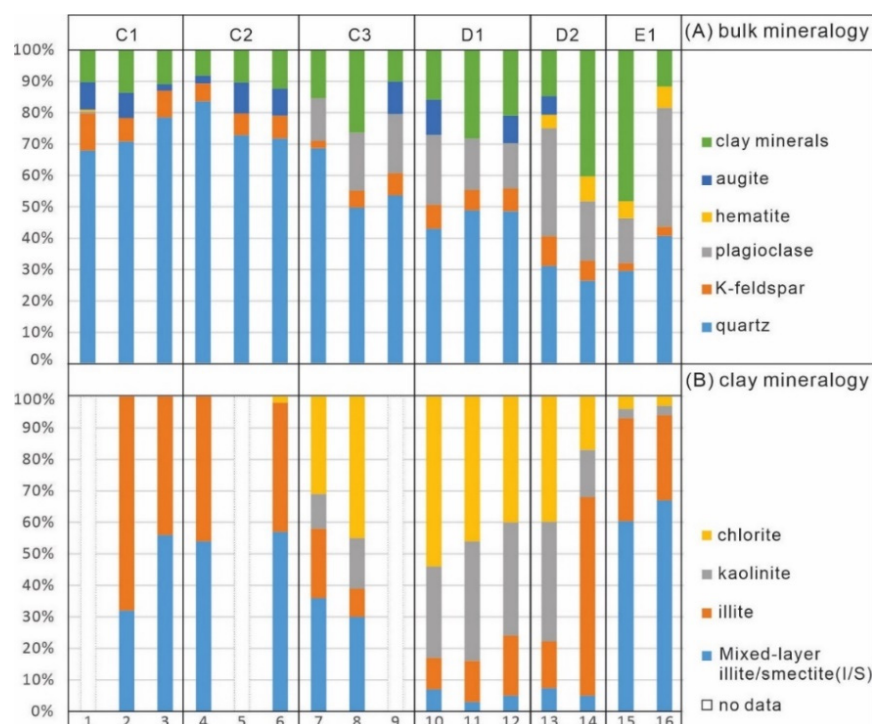
Figure 6. XRD major and clay mineral components.

5. Discussion

5.1. Depositional Age of the Thick Sandy Conglomerates from Borehole BZ26-A

Due to the lack of biostratigraphic information and syn-depositional volcanic layers, the depositional age of the sandy conglomerate could be achieved through constraints of absolute ages of minerals and correlation with well-understood samples. On one hand, the formation of tectonic fissures and following diagenesis took place after deposition, which suggests the time of secondary mineral precipitation could offer an upper bound for the depositional age. On the other hand, the detrital zircons in the sandy conglomerate were derived from the source areas, which crystallized before the deposition of the strata. Therefore, the youngest detrital zircon age could constrain the maximum depositional age [8,9].

The in situ U-Pb dating yields a major vein calcite age of 47.0 Ma, which falls in the time interval of 50.5–42.0 Ma, corresponding to the fourth member of the Shahejie Formation (Es$_4$) [13]. It indicates that the calcite precipitated synchronously with the deposition of Es$_4$ and the host rock of thick sandy conglomerates is supposed to be older than Es$_4$ and more likely to be part of the Kongdian Formation. However, it is worth noting that the narrow range of $^{238}U/^{206}Pb$ yields relatively high uncertainty, which makes the constraint less confident and it also indicates that the in situ U-Pb dating of carbonate minerals in clastic rocks remains a technical challenge.

The detrital zircon ages of the sandy conglomerates correspond well to the base rocks in the Bohai Bay Basin exposed on adjacent uplifts. It is composed of Precambrian grains with peaks at 2506 Ma and 1877 Ma, respectively, corresponding to the dominated age clusters in the North China Block [23–26], and the Mesozoic grains with a major peak at 120 Ma, corresponding to the Yanshanian tectonic event [27,28] (Deng et al., 2007; Wang et al., 2018) (Figure 5). The youngest age, 103.5 Ma, suggests no Cenozoic zircon grains were detected in the detrital zircons, and the strata are supposed to be deposited after 103.5 Ma, which provides a wide lower-bound constraint. Therefore, the depositional age of the sandy conglomerate sequence falls into the time interval of 103.5 Ma to 47.0 Ma. Combined with the Cenozoic geological setting, the sandy conglomerate sequence is more likely to be part of the Kongdian Formation, similar to those deposited in the BZ19-6 structure.

In addition, in the east of Bonan Low Uplift and Central Structural Belt, two boreholes with cores drilled into the Kongdian Formation and the distinguished red to brown deposits offer relatively continuous depositional records to compare. The mineral components in the matrix of the conglomerates are an integrated reflection of the source system in a certain period, which offers another proxy for the stratigraphic correlation.

5.2. Mineralogy of Kongdian Formation in Huanghekou Sag

As revealed by previous studies and the detrital zircon analysis in this study, the pre-Cenozoic basement consisting of Archaean–Proterozoic meta-granites, Early Paleozoic carbonate, and Mesozoic volcanic rocks from bottom to top, which were exposed on the Bonan Low Uplift, provided the sedimentary materials that were deposited in northern Huanghekou Sag [29]. The erosional process in chronological order under variable climate is supposed to be recorded by the sediments and could be traced by the change in major minerals of quartz, K-feldspar, plagioclase, and augite derived from the source area, and hematite, an indicator of climate.

The mineral components in the inter-gravel matrix from the sandy conglomerates are integrated reflections of the provenance system in a certain period. As shown in Figure 6, the XRD data could be well organized and divided into several groups. The red to brown strata of cores D1 from BZ28-A and E1 from BZ34-A are considered as the mark of the Kongdian Formation, where hematite (4–8%) is the cause of the color, reflecting a hot and dry climate [14]. Samples from core D1 (BZ28-A) and C3 (BZ26-A) show no hematite but approximately 20% of plagioclase, which is absent in the samples from C1 and C2 intervals of BZ26-A. The high contents of quartz and low contents of plagioclase from C1 and C2 suggest enhanced sources from the Precambrian meta-granites compared with the Mesozoic volcanic rocks with high plagioclase phenocrysts. The clay mineral analysis suggests a similar trend, where samples from D1, D2, and C3 show higher contents of chlorite than C1 and C2, which might be the result of the dissolution of Mesozoic volcanic rocks.

5.3. Implication on the lithostratigraphy of Kongdian Formation in Huanghekou Sag

The in situ U-Pb dating of both vein calcite and detrital zircons provides the upper and lower bounds of the depositional age of the sandy conglomerates, accumulated in the northern steep slope zone of Huanghekou Sag. Combined with the XRD mineral analysis, the lithostratigraphic units of the Kongdian Formation in Huanghekou Sag could be subdivided into at least three members (Table 1).

Table 1. Schematic correlation chart of the Kongdian Formation in Huanghekou Sag.

Kongdian Fm.	Geochronologic Constraints	Diagnostic Characteristics	Unknown BZ26-A	Known BZ28-A	Known BZ34-A
Member 1	(1) Vein Calcite age = 47 ± 14.3 Ma (2) Youngest detrital zircon age = 103.5 ± 2.5 Ma	(1) High quartz and K-feldspar with low plagioclase (2) Major provenance of Precambrian meta-granites	C1 and C2		
Member 2		(1) High plagioclase and high clay minerals (2) Major provenance of Mesozoic volcanic rocks	C3	D1	
Member 3		(1) Red to brown strata (2) Hot and dry climate		D2	E1

Member 3 of the Kongdian Formation was deposited in a hot and dry climate when the Huanghekou Sag was characterized by separated uplifts and depressions, with deposition of alluvial fans of red to brown sandy conglomerates. With the expansion of the lacustrine

basin and enhanced faulting activity, fan delta deposited at the northern steep slope zone, with materials mainly from erosion of the Mesozoic volcanic rocks on Bonan Low uplifts. Weathering and dissolution of the volcanic material resulted in high contents of plagioclase and clay minerals of kaolinite and chlorite in the following diagenesis of Member 2. Further erosion of Bonan Low Uplift exposed larger areas of the Precambrian meta-granitoid, whose erosion offered large amounts of quartz and feldspar grains and low-clay-mineral content in the sandy conglomerates of Member 1.

5.4. Exploration Potential of the Kongdian Formation in Huanghekou Sag

The discussion above suggests the Kongdian Formation deposited in the steep slope zone of Bonan Low Uplift is characterized by internal subdivision with inhomogeneous mineral composition. Unlike Member 2 and Member 3 of the Kongdian Formation, drilled by borehole BZ28-A and BZ34-A in the east and Central Structural Belt, cores C1 and C2 represent Member 1 of the Kongdian Formation, with dominant quartz and low clay contents. The high contents of brittle minerals enhanced the development of the tectonic fissures, which significantly improve the permeability of the sandy conglomerate sequence under the background of intense fault activities. It is supposed that the sandy conglomerates of Member 1 of the Kongdian Formation in the steep slope zone of Huanghekou Sag might be of significant potential for oil and gas exploration.

6. Conclusions

In this study, we reported one U-Pb age of vein calcite and 235 detrital zircon ages of sandy conglomerate samples from borehole BZ26-A and conducted XRD analysis on samples from both BZ26-A and two well-understood boreholes of BZ28-A and BZ34-A. Based on the data and comparison, we draw two key conclusions:

(1) The absolute age of 47 ± 14.3 Ma of the vein calcite and the 103.5 ± 2.5 Ma of the youngest detrital zircon age suggest the thick sandy conglomerate sequence (~160 m in thickness) accumulated in the steep slope zone of Huanghekou Sag is supposed to be part of the Kongdian Formation, similar to those developed in the BZ19-6 Structure.

(2) Lithostratigraphy of the Kongdian Formation in Huanghekou Sag could be subdivided into at least three lithostratigraphic members with Member 3 consisting of red to brown sediment, deposited in a hot and dry climate, while Member 2 and Member 1 were deposited in fan delta facies, with major sediments from Mesozoic volcanic rocks and Precambrian meta-granitoid exposed on Bonan Low Uplift, respectively. Member 1 shows significant potential for further exploration.

References

1. Shi, H.S.; Wang, Q.B.; Wang, J.; Liu, X.J.; Feng, C.; Hao, Y.W.; Pang, W.J. Discovery and exploration significance of large condensate gas fields in BZ19-6 structure in deep Bozhong sag. *China Pet. Explor.* **2019**, *24*, 36–45, (In Chinese with English abstract).
2. Du, X.F.; Wang, Q.M.; Zhao, M.; Liu, X.J. Sedimentary characteristics and mechanism analysis of a large-scale fan delta system in the Paleocene Kongdian Formation, Southwestern Bohai Sea, China. *Interpretation* **2020**, *8*, SF81–SF94. [CrossRef]
3. Li, C.; Zhang, J.; Song, M.; Shi, C.; Shi, N.; Liu, T. Fine division and correlation of glutenite sedimentary periods based on sedimentary facies in version-A case study from the Paleogene strata of upper Es4 in the Yanjia Area, Dongying Depression. *Acta Geol. Sin.* **2011**, *85*, 1008–1018, (In Chinese with English abstract).
4. Cao, J.; Luo, J.; Ma, M.; Sheng, W.; Mao, Q.; Yang, T.; Di, W.; Song, K. Influence mechanism of micro-heterogeneity on conglomerate reservoir densification: A case study of Upper Permian Wutonggou Formation in DN8 Area of Dongdaohaizi Sag, Junggar Basin. *Earth Sci.* **2021**, *46*, 3435–3452.
5. Coogan, L.A.; Parrish, R.R.; Roberts, N.M.W. Early hydrothermal carbon uptake by the upper oceanic crust: Insight from in situ U-Pb dating. *Geology* **2016**, *44*, 147–150. [CrossRef]
6. Hansman, R.J.; Albert, R.; Gerdes, A.; Ring, U. Absolute ages of multiple generations of brittle structures by U-Pb dating of calcite. *Geology* **2018**, *46*, 207–210. [CrossRef]
7. Su, A.; Chen, H.H.; Feng, Y.X.; Zhao, J.X.; Nguyen, A.D.; Wang, Z.C.; Long, X.P. Dating and characterizing primary gas accumulation in Precambrian dolomite reservoirs, Central Sichuan Basin, China: Insights from pyrobitumen Re-Os and dolomite U-Pb geochronology. *Precambrian Res.* **2020**, *350*, 105897. [CrossRef]
8. Fedo, C.M.; Sircombe, K.; Rainbird, R. Detrital zircon analysis of the sedimentary record. *Rev. Mineral. Geochem.* **2003**, *53*, 277–303. [CrossRef]
9. Anderson, T. Detrital zircons as tracers of sedimentary provenance: Limiting conditions from statistics and numerical simulation. *Chem. Geol.* **2005**, *216*, 249–270. [CrossRef]
10. Gehrels, G. Detrital zircon U-Pb geochronology: Current methods and new opportunities. In *Tectonics of Sedimentary Basins: Recent Advances*; Busby, C., Azor, A., Eds.; Blackwell Publishing: Chichester, UK, 2012; pp. 45–62.
11. Qi, J.; Yang, Q. Cenozoic structural deformation and dynamic processes of the Bohai Bay basin province, China. *Mar. Pet. Geol.* **2010**, *27*, 757–771. [CrossRef]
12. Feng, Y.; Jiang, S.; Hu, S.; Li, S.; Lin, C.; Xie, X. Sequence stratigraphy and importance of syndepositional structural slope-break for architecture of Paleogene syn-rift lacustrine strata, Bohai Bay Basin, E. *China. Mar. Pet. Geol.* **2016**, *69*, 183–204. [CrossRef]
13. Qiu, N.; Zuo, Y.H.; Xu, W.; Li, W.Z.; Chang, J.; Zhu, C.Q. Meso-Cenozoic lithosphere thinning in the eastern North China Craton: Evidence from thermal history of the Bohai Bay Basin, North China. *J. Geol.* **2016**, *124*, 195–219. [CrossRef]
14. Li, J.P.; Zhou, X.H.; Liu, S.L.; Zhang, Y.H. On the distribution of the Kongdian Formation in the Bohai area with special reference to its bearings on oil exploration. *J. Stratigr.* **2010**, *34*, 89–96. (In Chinese with English abstract)
15. Yang, H.; Qian, G.; Xu, C.; Gao, Y.; Kang, R. Sandstone distribution and reservoir characteristics of Shahejie Formation in Huanghekou Sag, Bohai Bay Basin. *Earth Sci.* **2022**. Available online: https://kns.cnki.net/kcms/detail/42.1874.p.20220228.1831.006.html (accessed on 2 March 2022). (In Chinese with English abstract)
16. Li, H.; Wang, Q.B.; Pang, X.Q.; Dai, L.M.; Liu, X.J. Fracture generation and reservoir evaluation of tight glutenite reservoir: A case study of second member of Shahejie Formation in Huanghekou Depression. *Geol. Sci. Technol. Inf.* **2019**, *38*, 176–185. (In Chinese with English abstract)
17. Nafi, M.; Fei, Q.; Yang, X.H. Type of sandstone and source of carbonate cement in the Kongdian Formation (Upper Part), South Slope of the Dongying Depression, East China. *J. Appl. Sci.* **2004**, *4*, 235–241. [CrossRef]
18. Paton, C.; Hellstrom, J.; Paul, B.; Woodhead, J.; Hergt, J. Iolite: Freeware for the visualization and processing of mass spectrometric data. *J. Anal. Atmos. Spectrom.* **2011**, *26*, 2508–2518. [CrossRef]
19. Vermeesch, P. Isoplot R: A free and open toolbox for geochronology. *Geosci. Front.* **2018**, *9*, 1479–1493. [CrossRef]
20. Wiedenbeck, M.; Alle, P.; Corfu, F.; Griffin, W.L.; Meier, M.; Oberli, F.; Vonquadt, A.; Roddick, J.C.; Speigel, W. Three natural zircon standards for U-Th-Pb, Lu-Hf, trace element, and REE analyses. *Geostand. Geoanalytical Res.* **1995**, *19*, 1–23. [CrossRef]
21. Sláma, J.; Kosler, J.; Condon, D.J.; Crowley, J.L.; Gerdes, A.; Hanchar, J.M.; Horstwood, M.S.A.; Morris, G.A.; Nasdala, L.; Norberg, N.; et al. Plesovice zircon—A new natural reference material for U–Pb and Hf isotopic microanalysis. *Chem. Geol.* **2008**, *249*, 1–35. [CrossRef]
22. Vermeesch, P. On the visualisation of detrital age distributions. *Chem. Geol.* **2012**, *312–313*, 190–194. [CrossRef]
23. Zhai, M.G.; Santosh, M. The early Precambrian odyssey of the North China Craton: A synoptic overview. *Gondwana Res.* **2011**, *20*, 6–25. [CrossRef]
24. Zhao, G.; Cawood, P.A.; Li, S.; Wilde, S.A.; Sun, M.; Zhang, J.; He, Y.; Yin, C. Amalgamation of the North China Craton: Key issues and discussion. *Precambrian Res.* **2012**, *222*, 55–76. [CrossRef]
25. Zhai, Y.; Gao, S.; Zeng, Q.; Chu, S. Geochronology, geochemistry and Hf isotope of the Late Mesozoic granitoids from the Lushi polymetal mineralization area: Implication for the destruction of Southern North China Craton. *J. Earth Sci.* **2020**, *31*, 313–329. [CrossRef]
26. Meng, F.; Tian, Y.; Kerr, A.C.; Wang, Q.; Chen, Y.; Zhou, Y.; Yang, F. Neoarchean reworking of Mesoarchean and Paleoarchean crust (3.4 ~ 3.0 Ga) within the North China Craton: Constraints from zircon U-Pb geochronology and Lu-Hf isotopes from the basement of the Bohai Bay Basin. *Precambrian Res.* **2022**, *369*, 106497. [CrossRef]

27. Deng, J.; Su, S.; Niu, Y.; Liu, C.; Zhao, G.; Zhao, X.; Wu, Z. A possible model for the lithospheric thinning of North China Craton: Evidence from the Yanshanian (Jura-Cretaceous) magmatism and tectonism. *Lithos* **2007**, *96*, 22–35. [CrossRef]
28. Wang, Y.; Sun, L.; Zhou, L.; Xie, Y. Discussion on the relationship between the Yanshanian Movement and cratonic destruction in North China. *Sci. China Earth Sci.* **2018**, *61*, 499–514. [CrossRef]
29. Pang, X.J.; Wang, Q.B.; Xie, T.; Zhao, M.; Feng, C. Paleogene provenance and its control on high-quality reservoir in the northern margin of Huanghekou Sag. *Lithol. Reserv.* **2020**, *32*, 1–13. (In Chinese with English abstract)